University of Bahrain
Journal of the Association of Arab Universities for Basic and Applied Sciences
www.elsevier.com/locate/jaaubas
www.sciencedirect.com

التوصيف التركيبي لمركب SiO_2/Zn_2SiO_4:Ce النانوي المحضر بطريقة المحلول الجلاتي

عزالدين شلوش، جمال جوادي، علي أكساس

مختبر البيئية الهندسي، جامعة بجاية، طريق أوزمور ثارقة، 06000، بجاية ،الجزائر

الملخص:

تم تحضير مسحوق أوكسيد الزنك المطعم بالسيليزيوم ومركب السليكا ZnO :Ce/SiO_2 النانوي بطريقة المحلول الجلاتي تحت التجفيف في الظروف الحرجة للإيثانول (درجة الحرارة و الضغط). تمت المعالجة الحرارية لمركب السليكا ZnO :Ce/SiO_2 النانوي عند درجة حرارة 1200°C تحت الضغط الجوي .لقد بينت قياسات حيود الأشعة السينية أن مسحوق أكسيد الزيك النانوي الذي تم تحضيره قد تبلور بطريقه جيدة من ناحية البنية السداسية وكان متوسط أبعاد حبيبات المسحوق تقدر بحوالي 78 نانومتر. كما ان الصور المجهرية قد بينت بأن البلورات تتكتل لتشكل كريات، او أشكال سداسية، أو أشكال سداسية محاطة بإطارات. إن ادخال أكسيد الزنك المطعم بالسيليزيوم ZnO :Ce الى السليكا يؤدي إلى تشكل سيليكات الزنك حتى قبل المعالجة الحرارية وان المعالجة تؤدي الى تناقص في انعكاسات حيود الأشعة السينية مما يدل على تعزيز تشكل سيليكات الزنك. فمنحنيات اللمعان الضوئي تبين أن ادخال ال ZnO :Ce الى السيلكا قبل المعالجه الحرارية يؤدي إلى تناقص في شدة الانبعاث الضوئي الفوق البنفسجي والى ازاحة مجمل طيف الانبعاث نحو الاشعة الحمراء. اما بعد المعالجة الحرارية، فشدة اللمعان الضوئي لمركب السليكا النانوي تناقصت بشكل ملحوظ.

Journal of the Association of Arab Universities for Basic and Applied Sciences (2014) **15**, 10–14

University of Bahrain

Journal of the Association of Arab Universities for Basic and Applied Sciences

www.elsevier.com/locate/jaaubas
www.sciencedirect.com

ORIGINAL ARTICLE

Structural characterization of SiO_2/Zn_2SiO_4:Ce nanocomposite obtained by sol gel method

A. Chelouche *, D. Djouadi, A. Aksas

Laboratoire de Génie de l'Environnement, Université de Béjaia, Route de Targa Ouzemmour, 06000 Béjaia, Algeria

Received 4 February 2013; revised 21 April 2013; accepted 5 May 2013
Available online 4 June 2013

KEYWORDS

ZnO:Ce;
ZnO:Ce/silica nanocomposite;
Zinc silicate;
Photoluminescence

Abstract Ce-doped ZnO nanopowder and ZnO:Ce/silica nanocomposite were synthesized by sol–gel process under supercritical drying (temperature and pressure) of ethanol. Annealing at 1200 °C under atmospheric pressure has been achieved for the prepared ZnO:Ce/silica nanocomposite. X-ray diffraction (XRD) showed good crystallinity and a ZnO hexagonal wurtzite structure of the as-prepared powder. The average crystallite size is of the order of 78 nm. Crystallites agglomerate to form spheres, hexagons and/or hexagons inserted in tori. The introduction of ZnO:Ce in silica leads to the formation of zinc silicate even before annealing. The heat treatment reduces the intensity of the diffraction peaks and enhanced the formation of this new phase. Photoluminescence (PL) spectra showed that the introduction of ZnO:Ce in silica before annealing reduces the UV lines and red shifts the entire emission. After annealing the PL intensity of the nanocomposite is significantly reduced.

1. Introduction

Recently, zinc oxide (ZnO) has attracted much interest because of its large exciton binding energy of 60 meV and a wide band-gap of 3.3 eV. This characteristic makes ZnO attractive for optoelectronic, nonlinear optics and electro-optics (Sahal et al., 2008), catalysts (Saad and Mary, 2008), active compounds in sunscreens applications (Smijs and Pavel, 2011). The ZnO structure contains large voids, which can easily accommodate interstitial atoms. It exhibits n-type semiconducting properties with inherent defects. The study of the photoluminescence (PL) characteristics of ZnO is interesting because it can provide valuable information on the quality and purity of the materials.

It is well known that chemical doping, as well as intrinsic lattice defects, greatly influences optical, electronic and magnetic properties of ZnO (Fujihara et al., 2004). Therefore, the doping of ZnO with selective elements offers an effective route to enhance and control its optical, electrical and magnetic properties, which is crucial for its practical application (Fang et al., 2011; Karaagac et al., 2012; Panigrahy and Bahadur, 2012). Doping with rare-earth (RE) offers a possible route for applications in high power lasers, visible emitting phosphors in displays and other optoelectronic devices. Cerium is a major element which has excellent luminescent properties and chemical sensor application (Dar et al., 2012; Anbia et al., 2012) when doped into matrix materials. As a dopant, Ce has received great attention due

* Corresponding author. Tel.: +213 556519868.
E-mail address: azeddinechelouche@gmail.com (A. Chelouche).
Peer review under responsibility of University of Bahrain.

ELSEVIER Production and hosting by Elsevier

1815-3852 © 2013 Production and hosting by Elsevier B.V. on behalf of University of Bahrain.
http://dx.doi.org/10.1016/j.jaubas.2013.05.002

to its peculiar optical and catalytic properties arising from the availability of the shielded 4f levels (Li et al., 2008; Yousefi et al., 2011) and the redox couple Ce^{3+}/Ce^{4+}.

Zinc silicate is a low cost material to adsorb toxic metal ions from water. Jin Qu et al. reported the flower-like and urchin-like morphology of zinc silicate nanomaterials produced by the hydrothermal method (Qu et al., 2012). Zn_2SiO_4 has been widely used as an important host material in cathode ray tubes (ElGhoul et al., 2010), electroluminescence devices, and light-emitting diodes (Wu et al., 2010). El Mir et al. fabricated zinc silicate and zinc oxide particles embedded in silica host matrix by the sol–gel method and they studied the emission properties of zinc silicate (El Mir et al., 2007). Li et al. synthesized $ZnO/Zn_2SiO_4/SiO_2$ composite pigments and studied the effects of α-Zn_2SiO_4 interface and its changes (Li et al., 2010).

In this paper we have reported the formation of zinc silicate phase and studied the photoluminescence behavior with annealing treatment.

2. Sample preparation

The monolithic silica matrix used in this work was obtained by mixing, under a constant magnetic stirring at room temperature, a tetraethoxysilane (TEOS), ethanol and distilled water. After 10 min of continuous agitation, a certain amount of hydrofluoric acid (HF) was added to the mixture. The wet gel obtained was finally dried in an autoclave.

ZnO:Ce aerogel powder was obtained by mixing, in adequate volume proportions, zinc acetate dehydrate ($Zn(C_2H_3O_2)_2$, $2H_2O$), under continuous magnetic stirring with ethanol and then a certain amount of cerium nitrate ($Ce(NO3)_3$, $6H_2O$) was added to the solution. The atomic ratio [Ce]/[Zn] is 2%. The final solution has undergone a drying in an autoclave under supercritical conditions of ethanol to obtain nano-sized powder of ZnO:Ce 2%.

The preparation of $ZnO:Ce/SiO_2$ nanocomposites was performed by dissolving TEOS in EtOH. Then the prepared ZnO:Ce powder was added to the mexture of TEOS and EtOH under constant stirring. The whole solution was stirred for about 30 min, resulting in the formation of a uniform sol. The sols were transferred to tubes in ultrasonic bath where a fluoride acid was added. The wet gel formed in a few seconds. Monolithic and white aerogel was obtained by supercritical drying. The drying is conducted at a temperature of 240 °C for 2 h and then were annealed for 2 h at a temperature of 1200 °C.

2.1. Sample characterization

The prepared ZnO:Ce powders and ZnO:Ce/SiO2 nanocomposites were characterized by X-ray diffraction (XRD) using a PanAnalytical diffractometer. X-rays are produced from a Cu Kα radiation source (wavelength λ = 1.5418 Å) with an acceleration voltage of 40 kV and a current of 30 mA.

Transmission electron microscopy images (TEM) were performed using a JEOLJEM-1230 TEM microscope with a very high acceleration voltage of the electron beam (110 kV). Scanning electron microscopy (SEM) images were performed with a JEOL JSM-840A. The photoluminescence spectrum was recorded at ambient temperature using a Perkin-Elmer LS55 spectrometer under excitation at 325 nm.

3. Results and discussions

Fig. 1a shows a SEM image of the Ce-doped ZnO aerogel. We note the coexistence of three morphologies: hexagons, spheres and hexagons inserted in tori. Spheres and tori average diameter is of the order of 5 μm. For hexagons, height and diameter are respectively 5 μm and 2.5 μm. We can suppose that the primary grain size of 78 nm agglomerates to form hexagons, spheres or tori inserted in the hexagons.

Fig. 1b shows a SEM image of $(ZnO:Ce)/SiO_2$ nanocomposite annealed at 1200 °C for 2 h in air. The above forms of ZnO:Ce aerogel are not existent and there is the appearance of new aggregates cylindrical in shape with a polygonal base. The annealing causes the interaction of ZnO and silica to form willemite (zinc silicate) which crystallized in a rhombohedra structure.

The TEM analysis of as prepared cerium-doped ZnO powder shows that the particles are in the nanoscale range (Fig. 2). The average crystallite size is 78 nm. This result confirms the XRD measurement below. We also note that some grains are hexagonal and others are triangular.

Fig. 3 shows XRD diagrams of ZnO:Ce aerogel, $ZnO:Ce/SiO_2$ nanocomposites before and after annealing at 1200 °C for 2 h. For ZnO:Ce aerogel (Fig. 3a), all diffraction peaks are characteristic of the hexagonal wurtzite ZnO with a slight shift toward smaller angles which is probably due to cerium (a = 0.3246 nm and c = 0.5212 nm) compared to those of

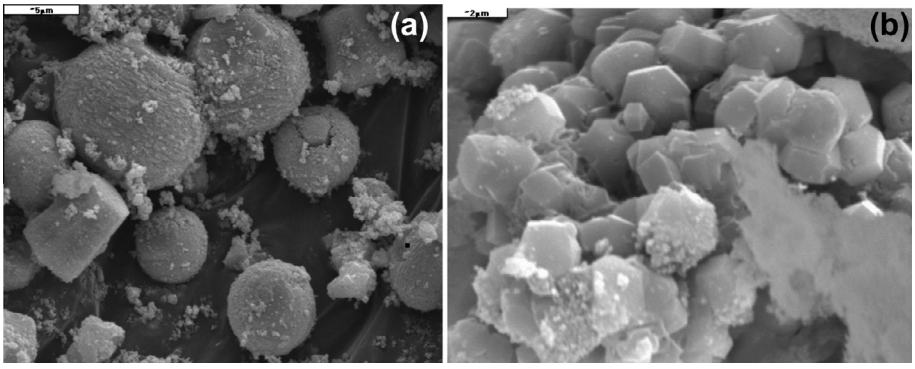

Figure 1 SEM images of ZnO:Ce aerogel (a) and $ZnO:Ce/SiO_2$ nanocomposite annealed at 1200 °C (b).

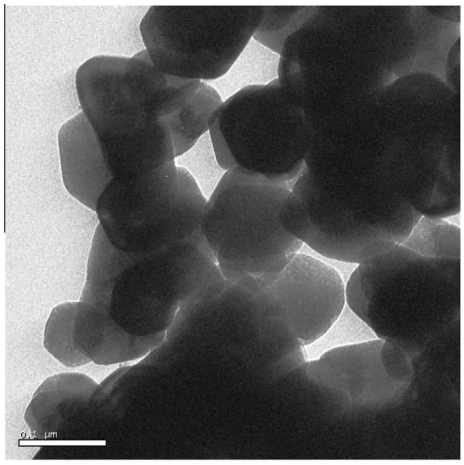

Figure 2 TEM image of ZnO:Ce aerogel.

pure ZnO (a = 0.3248 nm, c = 0.5201 nm) (Djouadi et al., 2010). It is also remarkable that no peak of cerium oxide is detected. The introduction of cerium in the ZnO lattice has not altered its crystalline structure. The average crystallite size of the ZnO:Ce aerogel, estimated by the Scherrer formula, is of the order of 78 nm.

The XRD diagram of ZnO:Ce/silica nanocomposite before annealing is showed in Fig. 3b. The intensity of diffraction peaks decreased sharply and some peaks disappeared completely. We also note the appearance of some relatively intense peaks at positions of 39° and 53°, which are probably due to the formation of zinc silicate (El Mir et al., 2007). We observe a slight shift to larger angles of ZnO characteristic peaks. This is due to the contraction of the lattice parameters induced by the small size of ZnO crystallites and the presence of structural defects in the material. ZnO:Ce nanocrystallites are homogeneously distributed in silica since the formation of the crystalline phase Zn_2SiO_4 from reactions between ZnO crystal and amorphous silica may occur at low temperatures when the crystallites of ZnO are well distributed in silica (Yang et al., 2002).

The XRD pattern of the ZnO:Ce aerogel introduced in a silica matrix and annealed at 1200 °C is shown in Fig. 3c. The intensity of the diffraction peaks is again amplified with increasing concentration of the crystallites. In addition to the

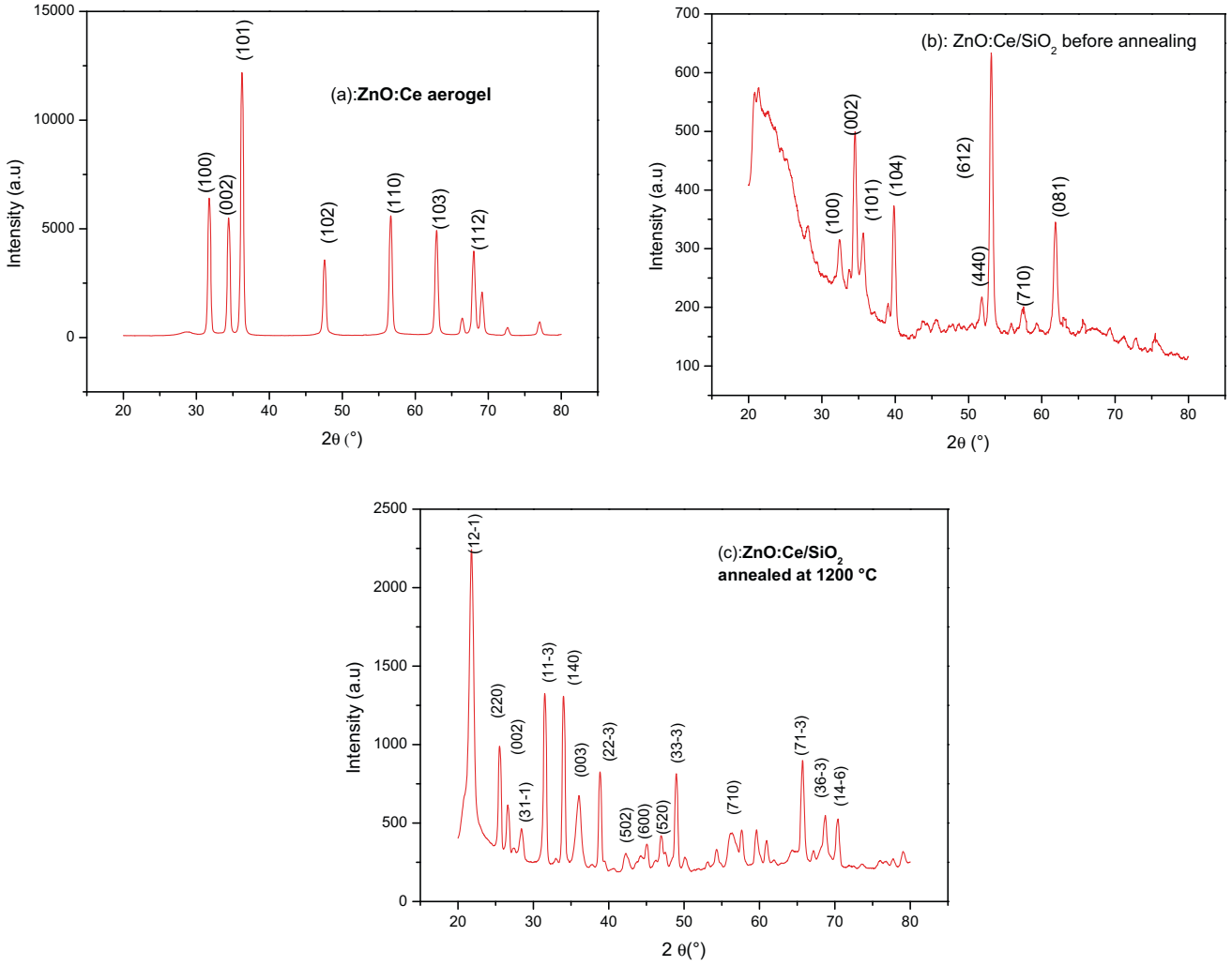

Figure 3 XRD diagrams of ZnO:Ce aerogel (a), ZnO:Ce/SiO_2 nanocomposite (b) and ZnO:Ce/SiO_2 nanocomposite annealed at 1200 °C (c).

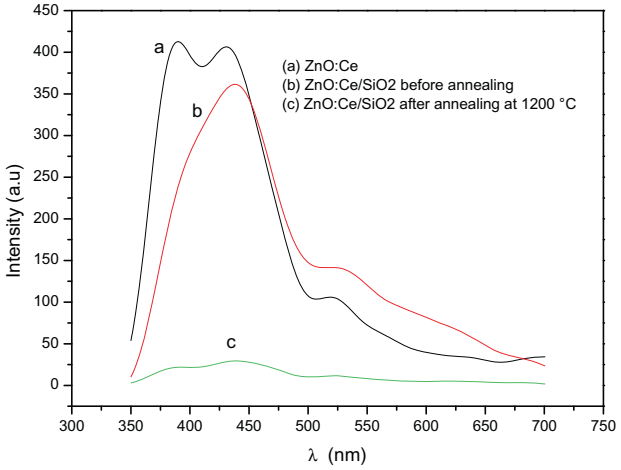

Figure 4 Photoluminescence spectra of ZnO:Ce (a), ZnO:Ce/SiO_2 (b) and Zn_2SiO_4:Ce (c).

ZnO characteristic peaks a slight offset to the small diffraction angles, those of different phases of zinc silicate (Zn_2SiO_4) are observed (cards JCPDS 00-024-1466 and 01-079-2005). There is a coexistence of ZnO:Ce and zinc silicate in the elaborated composite. The Zn and Si elements at the surface of the silica are susceptible to move and diffuse into the pores to form zinc silicate (El Mir et al., 2007).

The photoluminescence spectra of ZnO:Ce aerogels and ZnO:Ce/SiO_2 nanocomposites before and after annealing are shown in Fig. 4. The photoluminescence spectrum at room temperature of ZnO:Ce aerogel (curve a) presents two lines centered around 390 and 440 nm in addition to a shoulder at 520 nm. The line at 390 nm is due to ZnO band to band emission. The band centered around 440 nm is attributed to cerium emission and the shoulder at 520 nm is the ZnO green luminescence.

It is noticeable that the introduction of ZnO:Ce in silica host decreased the UV emission at 390 nm and became a shoulder. Also, a red shift is observed. This feature can be explained by the fact that the energy levels of Ce^{3+} are affected by the surrounding medium. The symmetry of crystals affects Ce^{3+} levels and the optical transitions are shifted from UV to visible in the different crystals. The increase in the Stokes shift gives rise to the broadening of emission bands. Thus, the emission bands become indistinguishable and appear as a single band (Sankar, 2008; Luo et al., 2012).

The nanocomposite annealed at 1200 °C (Fig. 4c) has a very low emission compared to that of the same nanocomposite before annealing (Fig. 4b), but the spectrum maintains its shape. It is well known that the intensity of the light emitted by cerium ions is proportional to their concentration. During heating, the Ce^{3+} ions are transformed into Ce^{4+} ions (Xu et al., 2007) and therefore a decrease of emitting centers concentration and consequently the intensity of the emitted light decreases considerably in the considered wavelength range where Ce^{4+} ions are inactive. After annealing at 1200 °C, the sample has red emission lines centered on 690 and 630 nm whose origin is independent of the presence of the rare earth ion but due to the emission of defects such as hole traps on oxygen and/or emission of zinc silicate crystallites formed during the heat treatment (El Mir et al., 2007).

4. Conclusion

We prepared ZnO:Ce aerogels and ZnO:Ce/silica nanocomposite by the sol–gel method under supercritical drying. The zinc silicate (Zn_2SiO_4) crystalline phase was obtained at room temperature from the reaction between ZnO and amorphous silica. ZnO:Ce primary crystallites agglomerate to form spheres, hexagons and hexagons inserted into tori. Silica modified the ZnO:Ce emission by reducing the UV band and red shifting the entire PL spectrum. Annealing causes a large decrease of PL intensity due to the transformation of Ce^{3+} to Ce^{4+}.

References

Anbia, M., Ebrahim, S., Fard, M., 2012. Humidity sensing properties of Ce-doped nanoporous ZnO thin film prepared by sol-gel method. J. Rare Earth 30, 38–42.

Dar, G.N., Umar, A., Zaidi, S.A., Ibrahim, A.A., Abaker, M., Baskoutas, S., Al-Assiri, M.S., 2012. Ce-doped ZnO nanorods for the detection of hazardous chemical. Sens. Actuat. B-Chem. 173, 72–78.

Djouadi, D., Aksas, A., Chelouche, A., 2010. Elaboration et Caractérisations structurales et optique de Nanocristallites toriques de ZnO. Ann. Chim-Sci. Mat (35/5), 255–260.

El Mir, L., Amlouk, A., Barthou, C., Alaya, S., 2007. Synthesis and luminescence properties of $ZnO/Zn_2SiO_4/SiO_2$ composite based on nanosized zinc oxide-confined silica aerogels. Physica B 388, 412–417.

ElGhoul, J., Barthou, C., Saadoun, M., ElMir, L., 2010. Optical characterization of SiO_2/Zn_2SiO_4:V nanocomposite obtained after the incorporation of ZnO:V nanoparticles in silica host matrix. J. Phys. Chem. Sol. 71, 194–198.

Fang, F., Zhao, D., Fang, X., Li, J., Wei, Z., Wang, S., Wu, J., Wang, X., 2011. Optical and electrical properties of individual p-type ZnO microbelts with Ag dopant. J. Mater. Chem. 21, 14979–14983.

Fujihara, S., Ogawa, Y., Kasai, A., 2004. Tunable visible photoluminescence from ZnO thin films through Mg-doping and annealing. Chem. Mater. 16, 2965–2968.

Karaagac, H., Yengel, E., Saif Islam, M., 2012. Physical properties and heterojunction device demonstration of aluminum-doped ZnO thin films synthesized at room ambient via sol–gel method. J. Alloys Compd. 521, 155–162.

Li, G.-R., Lu, X.-H., Zhao, W.-X., Su, C.-Y., Tong, Y.-X., 2008. Controllable electrochemical synthesis of Ce^{4+}-doped ZnO nanostructures from nanotubes to nanorods and nanocages. Cryst. Growth Des. 8 (4), 1276–1281.

Li, C., Liang, Z., Xiao, H., Wu, Y., Liu, Y., 2010. Synthesis of $ZnO/Zn_2SiO_4/SiO_2$ composite pigments with enhanced reflectance and radiation-stability under low-energy proton irradiation. Mater. Lett. 64, 1972–1974.

Luo, Q., Wang, L.S., Guo, H.Z., Lin, K.Q., Chen, Y., Yue, G.H., Peng, D.L., 2012. Blue luminescence from Ce-doped ZnO thin films prepared by magnetron sputtering. Appl. Phys. A 108, 239–245.

Panigrahy, B., Bahadur, D., 2012. P-type phosphorus doped ZnO nanostructures: an electrical, optical, and magnetic properties study. RSC Advances 2, 6222–6227.

Qu, J., Cao, C.-Y., Hong, Y.-L., Chen, C.-Q., Zhu, P.-P., Song, W.-G., Wu, Z.-Y., 2012. New hierarchical zinc silicate nanostructures and their application in lead ion adsorption. J. Mater. Chem. 22, 3562–3567.

Saad, L., Mary, R., 2008. Characterization of various zinc oxide catalysts and their activity in the dehydration–dehydrogenation of isobutanol. J. Serb. Chem. Soc. 73 (6), 997–1009.

Sahal, M., Hartiti, B., Ridah, A., Mollar, M., Marı, B., 2008. Structural, electrical and optical properties of ZnO thin films deposited by sol-gel method. Microelectr. J. 39 (12), 1425–1428.

Sankar, R., 2008. Efficient blue luminescence in Ce3 + -activated borates, A6MM′(BO3)6. Solid State Sci. 10, 1864–1874.

Smijs, T.G., Pavel, S., 2011. Titanium dioxide and zinc oxide nanoparticles in sunscreens: focus on their safety and effectiveness. Nanotech. Sci. Appl. 4, 95–112.

Wu, Y., Wang, Y., He, D., Fu, M., Chen, Z., Li, Y., 2010. Spherical Zn_2SiO_4:Eu^{3+}@SiO_2 phosphor particles in core–shell structure: synthesis and characterization. J. Lum. 130, 1768–1773.

Xu, G.Q., Zheng, Z.X., Tang, W.M., Wu, Y.C., 2007. Multi-peak behavior of photoluminescence of silica particles heat-treated in hydrogen at elevated temperature. J. Lum 126, 43–47.

Yang, P.K., Lu, M., Song, C.F., Liu, S.W., Yuan, D.R., Xu, D., Gu, F., Cao, D.X., Chen, D.H., 2002. Preparation and characteristics of sol–gel derived Zn_2SiO_4 doped with Ni^{2+}. Inorg. Chem. Commun. 5, 482–486.

Yousefi, M., Azimirad, R., Amiri, M., Moshfegh, A.Z., 2011. Effect of annealing temperature on growth of Ce-ZnO nanocomposite thin films: X-ray photoelectron spectroscopy study. Thin Solid Films 520, 721–725.